The effects of deep convection on the concentration and size distribution of aerosol particles within the upper troposphere: A case study

Yan Yin,[1] Qian Chen,[1] Lianji Jin,[2] Baojun Chen,[3] Shichao Zhu,[1] and Xiaopei Zhang[1]

Received 23 March 2012; revised 12 September 2012; accepted 7 October 2012; published 16 November 2012.

[1] A cloud resolving model coupled with a spectral bin microphysical scheme was used to investigate the effects of deep convection on the concentration and size distribution of aerosol particles within the upper troposphere. A deep convective storm that occurred on 1 December, 2005 in Darwin, Australia was simulated, and was compared with available radar observations. The results showed that the radar echo of the storm in the developing stage was well reproduced by the model. Sensitivity tests for aerosol layers at different altitudes were conducted in order to understand how the concentration and size distribution of aerosol particles within the upper troposphere can be influenced by the vertical transport of aerosols as a result of deep convection. The results indicated that aerosols originating from the boundary layer can be more efficiently transported upward, as compared to those from the mid-troposphere, due to significantly increased vertical velocity through the reinforced homogeneous freezing of droplets. Precipitation increased when aerosol layers were lofted at different altitudes, except for the case where an aerosol layer appeared at 5.4–8.0 km, in which relatively more efficient heterogeneous ice nucleation and subsequent Wegener-Bergeron-Findeisen process resulted in more pronounced production of ice crystals, and prohibited the formation of graupel particles via accretion. Sensitivity tests revealed, at least for the cases considered, that the concentration of aerosol particles within the upper troposphere increased by a factor of 7.71, 5.36, and 5.16, respectively, when enhanced aerosol layers existed at 0–2.2 km, 2.2–5.4 km, and 5.4–8.0 km, with Aitken mode and a portion of accumulation mode (0.1–0.2 μm) particles being the most susceptible to upward transport.

Citation: Yin, Y., Q. Chen, L. Jin, B. Chen, S. Zhu, and X. Zhang (2012), The effects of deep convection on the concentration and size distribution of aerosol particles within the upper troposphere: A case study, *J. Geophys. Res.*, *117*, D22202, doi:10.1029/2012JD017827.

1. Introduction

[2] The upper troposphere (UT) plays an important role in chemistry-climate coupling and the radiative forcing of the climate system [*Shepherd*, 2007]. Aerosol particles uplifted to this layer could affect the radiative balance by direct scattering and the absorption of solar and terrestrial radiation, or can modify cloud optical properties by acting as cloud condensation nuclei (CCN) and ice nuclei (IN) [*Zhang et al.*, 1998; *Ekman et al.*, 2004; *Yin et al.*, 2005; *Wu et al.*, 2011]. From CALIPSO lidar measurements, *Vernier et al.* [2011] noticed the persistence of an aerosol layer at the level of the tropopause within the Asian monsoon region, and suggested that it may have an important impact on the radiative and chemical balance of the global UT.

[3] Deep convective clouds provide an efficient mechanism for pumping aerosol particles from the planetary boundary layer into the UT [*Cui and Carslaw*, 2006; *Hermann et al.*, 2008; *Froyd et al.*, 2009; *Fierli et al.*, 2011]. Using numerical simulation, *Wu et al.* [2011] pointed out that biomass burning aerosols may significantly warm the UT through local radiative heating when uplifted into this layer by deep convection, and can lead to significant moistening in the UT. *Su et al.* [2011] verified this result by determining that the increase in water vapor within the tropical tropopause was closely correlated to the enhancement of the particle population. *De Reus et al.* [2001] also provided evidence and found that elevated nucleation mode particles in the layer between 8 and 12.5 km originated from

[1]CMA Key Laboratory for Atmospheric Physics and Environment, Nanjing University of Information Science and Technology, Nanjing, China.
[2]Key Laboratory of Meteorological Disaster of Ministry of Education, Nanjing University of Information Science and Technology, Nanjing, China.
[3]Key Laboratory of Mesoscale Severe Weather, and School of Atmospheric Sciences, Nanjing University, Nanjing, China.

Corresponding author: Y. Yin, CMA Key Laboratory for Atmospheric Physics and Environment, Nanjing University of Information Science and Technology, 219 Ningliu Rd., Nanjing 210044, China. (yinyan@nuist.edu.cn)

0148-0227/12/2012JD017827

the outflow of large convective clouds during the Indian Ocean Experiment (INDOEX). On the other hand, *Andreae et al.* [2001] indicated that deep convective clouds could effectively scavenge most of the aerosol particles of accumulation mode, but could also allow the vertical transport of Aitken mode particles to the cloud top. *Ekman et al.* [2004, 2006] also reached similar conclusions based on numerical simulations.

[4] During vertical transport, aerosol particles can have an important impact on dynamic and microphysical processes, as well as on precipitation formation in convective clouds. Many previous studies have considered the response of convective cloud properties and precipitation to changes in the number concentration and the size distribution of background aerosol particles [e.g., *Yin et al.*, 2002; *Khain and Pokrovsky*, 2004; *Lee and Feingold*, 2010; *Chen and Yin*, 2011]. Several studies indicate that the responses of cloud parameters and precipitation amount to changes in the concentration of aerosol particles were nonlinear, and that either the updrafts or precipitation may increase or decrease depending on the CCN concentration, as well as environmental atmospheric conditions [*Ekman et al.*, 2007; *Zhang et al.*, 2009; *Fan et al.*, 2007; *Lee et al.*, 2008, 2009; *Ntelekos et al.*, 2009; *Martins et al.*, 2009; *Chen et al.*, 2011]. Therefore, the response of aerosol properties within the UT to vertical transport by deep convection may vary with different background aerosol conditions and the altitude of the aerosol particles being transported.

[5] In the present study, a cloud resolving model, coupled with a spectral bin microphysical scheme, was used to investigate the effects of deep convection on the concentration and size distribution of aerosol particles within the upper troposphere. A two-dimensional spectral resolving cloud model was utilized, and special attention was paid to the impact of aerosol layers at different altitudes on the characteristics of the aerosols within the UT, due to deep convection and physical mechanisms during transport.

[6] The paper is organized as follows: In section 2, the model description and the initialization are provided. In section 3, the dynamics and the microphysics of the simulated thunderstorm are compared to available measurements, and followed by sensitivity tests in order to investigate the response of aerosol properties within the UT to aerosol layers originating at different altitudes. A summary and conclusions are presented in section 4.

2. The Model Description and the Setup of Numerical Experiments

2.1. The Numerical Framework

[7] To represent deep convection, the two-dimensional cloud-resolving model (CRM) [*Tao et al.*, 2003] developed at NASA/GSFC was chosen as the dynamic framework [*Johnson et al.*, 2002]. Detailed equations for the dynamic processes included in the CRM are described by *Soong and Ogura* [1980], *Soong and Tao* [1980], and *Tao and Simpson* [1993]. The parameterization for subgrid-scale (turbulence) processes was based on *Klemp and Wilhelmson* [1978] and *Soong and Ogura* [1980]. The effect of condensation on the generation of subgrid-scale kinetic energy was also incorporated into the model based on *Tao and Simpson* [1993].

[8] The spectral (bin) microphysical scheme for cloud processes developed at Tel Aviv University [*Tzivion et al.*, 1987; 1989; *Feingold et al.*, 1988; *Reisin et al.*, 1996; *Yin et al.*, 2000], and the liquid-phase chemical processes of *Yin et al.* [2005] were adopted, allowing horizontal and vertical transport and diffusion, as well as the impaction scavenging of aerosol particles by cloud particles. Four species of hydrometeors are considered in the model, as follows: liquid drops, ice crystals, graupel particles, and aggregates (snowflakes).

[9] In this study, a new parameterization approach for heterogeneous ice nucleation, as proposed by *DeMott et al.* [2010], was introduced in the model. The approach considers the influence of the concentration of aerosol particles on the concentration of ice nuclei. Therefore, the concentration of ice particles nucleated at the grid point was constrained not only by temperature and water vapor, as in previous models, but also by the concentration of aerosol particles available at that location.

[10] The computational domain was comprised of 1,024 $\times$ 33 grid points with a horizontal resolution of 1 km. Separate numerical tests with a grid size of 750 m indicated that, with the exception of a 7-min advance in cloud formation, main characteristic values such as maximum updraft and the peak radar echo are generally similar to that reported in this paper, also agreed with the conclusion of *Bryan and Morrison* [2012] that convective clouds with a larger horizontal grid spacing are slower to develop. There are 33 stretched vertical levels with a resolution ranging from 200 m near the surface to approximately 1 km at the uppermost model level. The time step was 5 s, and the total integration time was 120 min in all of the runs.

2.2. Design of the Numerical Experiments

[11] A deep convective event that occurred on 1 Dec 2005 in Darwin, Australia, during the Stratospheric-Climate Links with Emphasis on the Upper Troposphere and Lower Stratosphere/Aerosol and Chemical Transport in Tropical Convection (SCOUT-O3/ACTIVE) field campaign, was simulated in this study. Figure 1 displays the profiles of the temperature and the dew point temperature as measured at the Darwin Airport (12.42°S, 130.89°E) at 23:00 UTC, 30 Nov 2005, which displays a very large convective available potential energy (CAPE) of approximately 1332 J kg^{-1}. The lapse rate of the temperature in the lowest 1.5 km was modified to 0.98 K/100 m to mimic the temperature profile when convection occurred [*Schafer et al.*, 2001]. In all of the numerical runs, convection was triggered by a warm bubble $\sim$30 km wide and 3 km deep, placed 1.5 km above the ground and at the horizontal center of the model domain. The maximum temperature perturbation was 3 K at the center of the bubble, with the amplitude decreasing in proportion to the square of the distance away from the center. The vertical and horizontal velocities of the wind were assumed to be zero at the initial time.

[12] The concentration and size distribution of background aerosol particles were based on the in situ measurements given by *Allen et al.* [2008] and *Qu* [2009], and are shown in Figure 2a in order to represent the average spectra of aerosol particles measured during the biomass burning season. Aerosol particles were assumed to be externally mixed and were composed of two species (i.e., water-soluble and

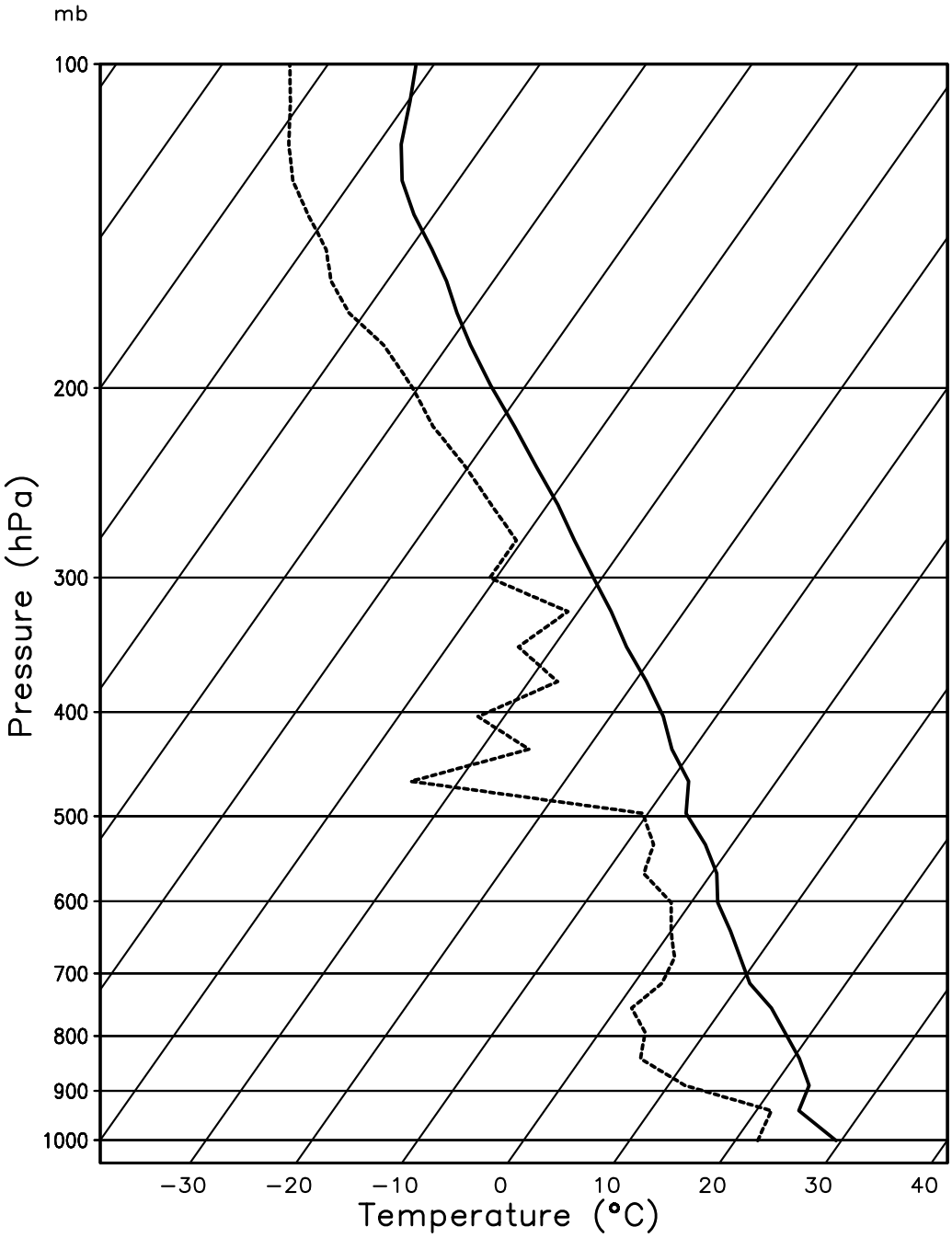

Figure 1. Profiles of temperature and dew point temperature at 23:00 UTC on 30 November 2005 at Darwin Airport (12.42°S, 130.89°E), Australia.

water-insoluble particles). Soluble particles were assumed to be composed of ammonium sulfate, regardless of size [*Yin et al.*, 2005]. In addition, the fraction of water-soluble material in background aerosol was assumed to be 24.96% of the total mass [*Allen et al.*, 2008], which could be removed by nucleation scavenging. Particles larger than 0.5 μm in diameter can also act as ice nuclei (IN) and participate in heterogeneous ice nucleation [*DeMott et al.*, 2010]. Since the concentration of these particles (usually less than 10^1 L^{-1} in the lower to mid- troposphere) are several orders of magnitude smaller than the total particle concentration (10^2 $\sim 10^6$ cm^{-3}), the depletion of dry aerosol particles by ice forming processes was ignored. The vertical profile of the concentration of aerosol particles below 4 km was determined based on the analysis of ACTIVE data by *Qu* [2009]. The particle concentration above 4 km was assumed to decrease exponentially with height (Figure 2b). The case simulated with the conditions mentioned above was named the CONTROL case.

[13] Depending on the synoptic conditions, aerosol particles can be transported to various altitudes [*Heald et al.*, 2006; *Tsai et al.*, 2008; *Stith et al.*, 2009]. To simulate the effect of aerosols lofted at different altitudes and the aerosol properties of the UT, aerosol layers were purposely added

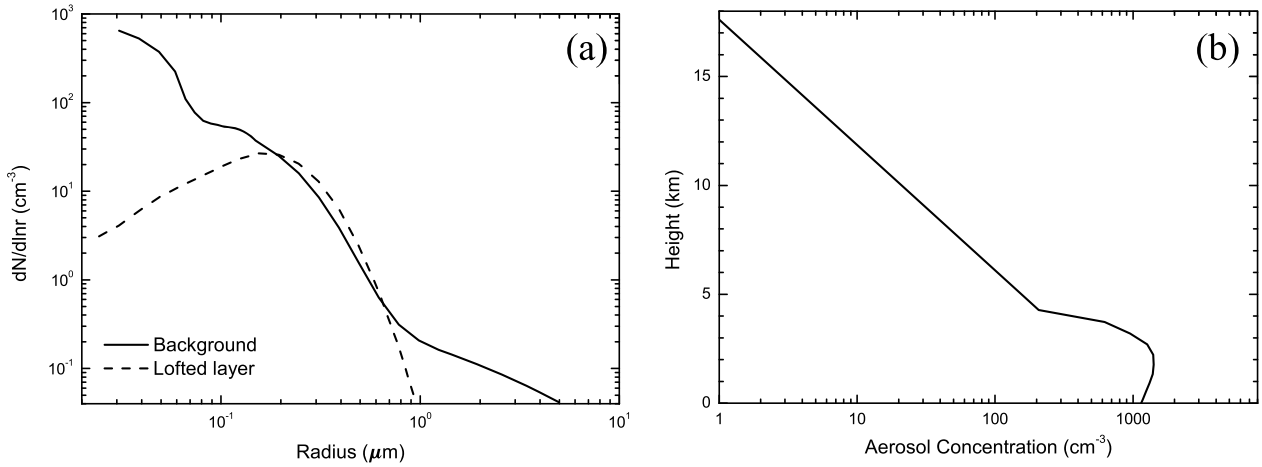

Figure 2. (a) Initial aerosol size distributions and (b) vertical profile of aerosol concentration.

at 0–2.2 km, 2.2–5.4 km, 5.4–8.0 km, 8.0–12.6 km, and 12.6–16.2 km, respectively, as shown in Figure 3, in order to resemble long-range transported aerosol layers at different altitudes. The cases are referred to as the LAYER1, LAYER2, LAYER3, LAYER4, and LAYER5 cases, respectively (Table 1). LAYER1 represents the situation (except for the background particle concentration) with additional aerosol pollution in the boundary layer. LAYER2 and LAYER3 were initialized with an aerosol layer in the mid-troposphere below 8 km; while the LAYER4 and LAYER5 cases represent situations for which aerosol layers were located above 8 km [*Devine et al.*, 2006]. The spectrum for aged aerosols observed by *Roberts et al.* [2006] was used as the input for the aerosol layers.

[14] To evaluate the response of simulated microphysical parameters for deep convective clouds to changes in aerosol layers, the population mean (the p-mean) of a given variable similar to that of *Wang* [2005b] and *Li et al.* [2008] was used to represent the averaged value over all qualified grids and during the entire simulation period.

3. Results and Discussions

3.1. Comparison With Radar Measurements

[15] Figure 4 provides the peak radar reflectivity simulated at 60 min for the CONTROL case, as compared with observations obtained by the C-band dual-polarization Doppler radar (C-Pol) at Gunn Point, just north of Darwin at 05:50 UTC. The major structure of the storm was well reproduced by the model, especially for the horizontal and vertical range of radar reflectivity larger than 50 dBz. However, the area with a weaker radar echo near the surface was not fully generated by the model, and the vertical extent of the radar echo simulated by the model was also slightly lower than the observations. The convective core (≥45 dBz) in the simulation appeared above 1 km, higher than the one observed. The approach of a warm bubble used to initialize the cloud may be partially responsible for discrepancies between modeled and measured radar reflectivity [*Li et al.*, 2008].

3.2. The Effect of Aerosol Layers on Clouds and Precipitation

[16] Figure 5 displays the time evolution of maximum updraft velocity for various cases. In the CONTROL case, the maximum vertical velocity peaked at 28 min in the simulation, and was related to the latent heat released during aerosol activation and the subsequent condensation growth

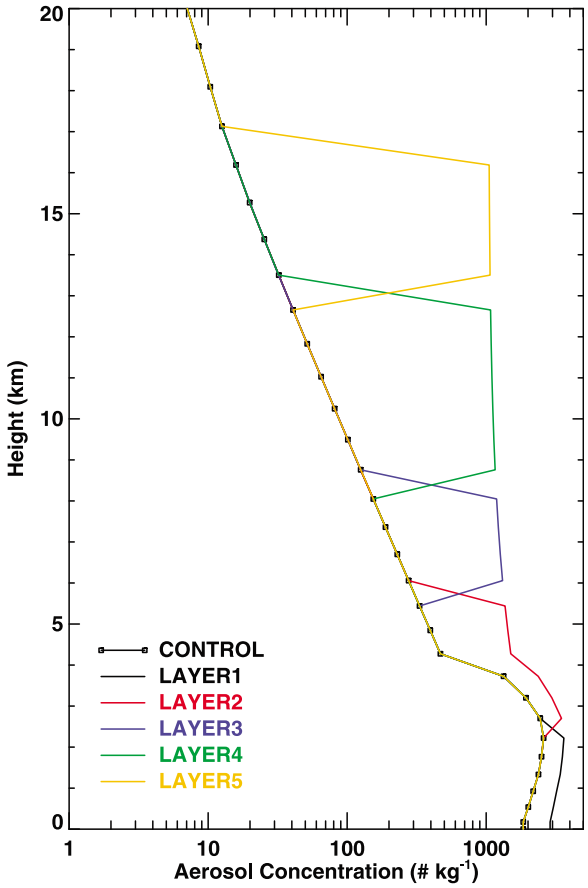

Figure 3. Vertical distribution of the concentration of aerosol particles at initial time.

Table 1. Summary of Sensitivity Experiments Conducted in This Study

Case	Brief Description
CONTROL	Without aerosol layer existing at any altitude
LAYER1	As CONTROL, with enhanced aerosol layer at altitude of 0–2.2 km
LAYER2	As CONTROL, with enhanced aerosol layer at altitude of 2.2–5.4 km
LAYER3	As CONTROL, with enhanced aerosol layer at altitude of 5.4–8.0 km
LAYER4	As CONTROL, with enhanced aerosol layer at altitude of 8.0–12.6 km
LAYER5	As CONTROL, with enhanced aerosol layer at altitude of 12.6–16.2 km

of water droplets from water vapor. During this stage, the cloud top reached approximately 7 km (Figure 6a). As a consequence of the homogeneous freezing of liquid droplets, the vertical velocity reached a secondary maximum value between 40 and 55 min. At this stage, the cloud had already developed to the altitude of 15 km (Figure 6b). The updraft slightly increased again after 65 min of simulation with the formation and rapid growth of graupel particles through the accretion of liquid drops. It should be noticed that the maximum vertical velocity at 28 min was larger than that at 75 min (Figure 5), but the wind vectors plotted in Figure 6b were longer than those in Figure 6a. This was caused by the stretched vertical grids of the model with coarse and fine resolution within the upper and lower levels, respectively.

[17] Similar to the CONTROL case, that the first increase in updraft velocity occurred from 28 to 38 min within the LAYER1 case was correlated with the efficient activation of aerosol particles lofted above the surface. With the help of the enhanced aerosol layer, the maximum concentration of droplets reached 637.8 cm^{-3} in the LAYER1 case, as compared to 442.4 cm^{-3} for the CONTROL case. The enhanced droplet concentration was then raised to higher altitudes and froze, resulting in the enhanced production of ice crystals and latent heat (Table 2), as well as an increased vertical velocity for the LAYER1 case from 40 to 50 min. The third peak of maximum vertical velocity that appeared from 64 to 90 min was most likely attributed to intensified graupel growth. For example, the maximum growth rates for graupel particles reached 0.01071 and 0.02879 g kg^{-1} s^{-1} at 75 min for the CONTROL and LAYER1 cases, respectively.

[18] In contrast, cloud dynamics and microphysical properties changed very little when aerosol layers existed at altitudes above the mid-troposphere, such as that for the LAYER2, LAYER3, LAYER4, and LAYER5 cases (Figure 5 and Table 2). The response of the updraft velocity to aerosol layers lofted at various altitudes is consistent with *Fan et al.* [2010], who pointed out that CCN in the lower troposphere were more important in modifying convection than those at other altitudes.

[19] Figure 7 displays changes in the cloud top height with time for various cases. As seen from the figure, the influence of aerosol layers on cloud top height is relatively small, even for the LAYER1 case. The result is inconsistent with some satellite observation analyses [e.g., *Choi et al.*, 2008; *Christensen and Stephens*, 2011], and is partly due to the fact that only a smaller number of aerosol particles are added at the boundary layer in the LAYER1 case as compared to the background particle concentration (Figure 2a). Also, as pointed out in other simulation studies [e.g., *Cui and Carslaw*, 2006; *Fan et al.*, 2012], the invigoration effect of CCN on deep convection clouds is not always obvious. It may also be possible that the changes in cloud top height resulting from relatively larger maximum updrafts from 60 to 80 min may not be well represented by Figure 5 due to the coarse vertical resolution close to the model top.

[20] For the cases modeled in this study, isotherms of 273 K and 235 K (homogeneous freezing level) were located at approximately 4.97 km and 10.62 km, respectively. Therefore, the aerosols added in the LAYER1 and LAYER2

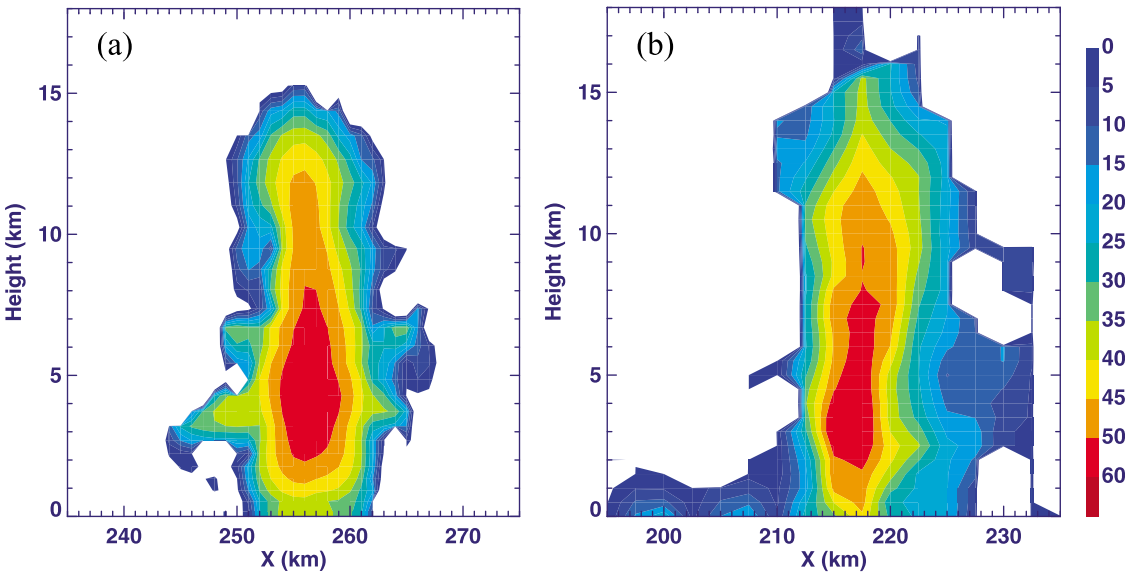

Figure 4. Radar reflectivity (in dBz) at the maximum developing stage obtained from (a) simulation and (b) observation.

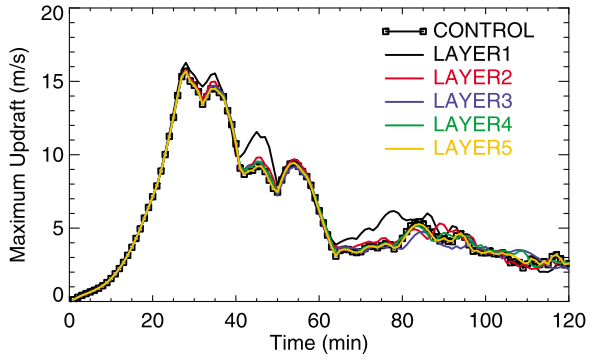

Figure 5. Time evolution of maximum updraft velocity for different experiments.

cases could act as CCN, and increase the number concentration of drops, as well as ice crystals, if they were homogeneously frozen. In contrast, the particles in the LAYER3 and LAYER4 cases mainly act as IN due to high altitudes and lower temperature. For the LAYER3 case, aerosol particles were added to the layer between 5.4 and 8.0 km, with the temperature ranging from 270 K to 254 K, a more suitable condition than in the LAYER4 case for the growth of ice particles via the Wegener-Bergeron-Findeisen mechanism [*Pruppacher and Klett*, 1997], leading to a decreased mean mass and number concentration for droplets due to an enhanced evaporation process (Table 2). In turn, due to the decreased number of drops available for graupel growth via accretion, a smaller graupel mass concentration resulted.

[21] As shown in Table 2, aerosols added in the LAYER5 case within the upper troposphere did not impact dynamic and microphysical processes. The p-mean values of the droplet number concentration in all of the simulated cases shown in Table 2 were lower as compared to other simulation studies [e.g., *Fan et al.*, 2007], since raindrops and cloud droplets were considered as one species in our model, and since fewer raindrops during the precipitation process led to smaller p-mean values for liquid drops.

[22] For deep convection, the response of precipitation to aerosol layers varied with the altitude of these aerosol layers (Figure 8). As compared to the CONTROL case, rainfall rates were larger when the aerosol concentration was enhanced at the boundary layer (the LAYER1 case). The result occurred due to the enhanced freezing of drops at higher altitudes and more melting precipitation, as discussed above, consistent with the simulation results of *Fan et al.* [2007], who also illustrated that higher aerosol concentrations result in stronger convection and more melting precipitation. The maximum rainfall rate also increased when aerosol layers existed at an altitude of 2.2–5.4 km and 8.0–12.6 km (for the LAYER2 and LAYER4 cases), but changed little when the aerosol layer appeared at 12.6–16.2 km (case LAYER5). It is interestingly noticed that the precipitation decreased when an aerosol layer located at 5.4–8.0 km (the LAYER3 case). This was caused by the smaller graupel mass mixing ratio (Table 2) with less melting rainfall, as discussed above. Simulation results shown by *Lebo and Seinfeld* [2011] demonstrated that with an increase in the IN number, the dynamic structure of deep convective clouds becomes small and may suppress precipitation. Different feedbacks for cloud microphysical and dynamic characteristics to lofted altitudes for the aerosol layers simulated here indicated a complicated relationship between aerosols and clouds.

3.3. The Variation of the Aerosol Concentration at Different Altitudes

[23] Figure 9 presents the time evolution of the mean concentration of aerosol particles at five altitudes (1.3 km, 3.7 km, 6.6 km, 10.2 km, and 14.4 km) for the CONTROL, LAYER1, LAYER2, LAYER3, LAYER4, and LAYER5 cases. The values were averaged over the horizontal between 220 and 290 km, the entire extent of the cloud. As seen in

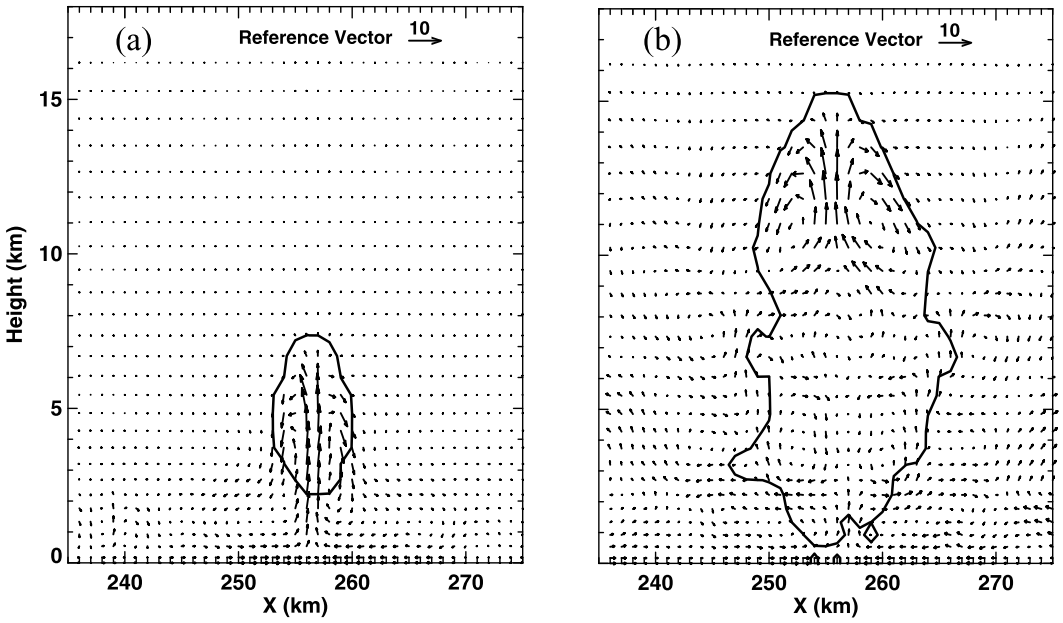

Figure 6. Wind field and the contours (0.01 g kg^{-1}) of mixing ratio of total hydrometers at (a) 28 min and (b) 55 min in case CONTROL.

Table 2. P-mean Values of Mass and Number Concentration of Droplets, Ice Crystals, and Graupel Particles in Different Cases[a]

Case	M_d (g kg^{-1})	M_i (g kg^{-1})	M_g (g kg^{-1})	N_d (cm^{-3})	N_i (L^{-1})	N_g (L^{-1})
CONTROL	0.37273	0.49804	0.80065	1.9710	617.66	1.1482
LAYER1	0.36797	0.56005	0.80523	2.2803	732.72	1.1887
LAYER2	0.37363	0.50679	0.79262	2.0479	653.57	1.1476
LAYER3	0.35877	0.48036	0.76218	1.9144	608.02	1.2036
LAYER4	0.37364	0.49969	0.79675	1.9847	625.16	1.1479
LAYER5	0.37279	0.49721	0.79492	1.9711	617.45	1.1439

[a]N and M stand for number and mass concentration with i, g and d corresponding to three hydrometer types (ice crystal, graupel and droplet), respectively.

Figure 9, the mean concentration of aerosol particles exhibited higher values within initial layers, and with the exception of values at 1.3 km the particle concentrations increased after 120 min of simulation. The mean particle concentrations at 3.7 km decreased for all cases from 20 to 40 min, corresponding to the appearance of the first peak updraft (Figure 5) that subsequently led to the enhancement of aerosol loading at an altitude of 6.6 km. A decrease in the particle number concentration at lower levels indicates that some of the particles were transported upward. Actually, this led to the significant accumulation of aerosol particles at altitudes of 10.2 km during the 35–50 min simulation. An increased vertical velocity from 50 to 60 min also resulted in particles being transported to altitudes of 14.4 km, especially in the LAYER4 case, for which an aerosol layer existed at 8.0–12.6 km. The aerosol concentration in the lower troposphere was maintained at initial values and changed little during the development and dissipation stage of the cloud due to the presence of background aerosol in the model that continually compensated for particles in the lower troposphere via the convergence process.

[24] The onset of impaction scavenging of aerosols by hydrometers exhibited a positive correlation with cloud top height (Figure 10). Maximum values for the impaction scavenging rate occurred at the altitude of 3.7 km for all simulations, and decreased with height. *Wang* [2005a] found that impaction scavenging was dominant within the lower and middle troposphere where the nucleation rate was relatively low. Scavenging rates for the two altitudes within the mid-troposphere (3.7 km and 6.6 km) increased again after 55 min, which corresponded to the stage with stronger precipitation (Figure 8). In Figure 8, one can also see that the scavenging rates were higher at their initial altitudes for the LAYER2, LAYER3, LAYER4, and LAYER5 cases, but had nearly no effect on scavenging rates near the surface (1.3 km).

3.4. Vertical Profiles of Aerosol Concentration

[25] Figure 11 provides the vertical profiles of the mean concentration of aerosol particles at the initial time and after 75 min of simulation. For the LAYER2 to LAYER5 cases, Figure 11 indicates that the particle concentrations in the original layers at 75 min were lower than that at the initial time, but at the level near the surface, the reverse was true, that is, the concentrations were higher at 75 min than that at the initial time, mainly due to the complement effect through the convergence process as mentioned above.

[26] Two peaks in values within the vertical profile of the aerosol concentration for the CONTROL case were evident. One peak appeared at the level of approximately 3–4 km (Figure 11b), and was related to the initial vertical profile. The other manifested itself at the level of 12–14 km, demonstrating the effect of upward transport by convection. For the LAYER1 case, due to the enhancement of aerosol loading near the surface at the initial time, the vertical profile only displayed one marked peak value at an altitude of 12–14 km. For the LAYER2 and LAYER3 cases, in which aerosol layers were present within the mid-troposphere, the vertical profiles had two peaks, one at the altitudes of their initial layers (at 3.7–5.4 km, and 6.1–8.0 km), and another that appeared at 12–14 km. An investigation of vertical transport in a mesoscale convective system by *Barthe et al.* [2011] also demonstrated two peaks in the vertical profiles for mid-tropospheric tracers. One peak was found at their initial layers, and the other was found at 13–14 km in altitude. The authors suggested that mid-tropospheric air is important for feeding the upper troposphere.

[27] Figure 11 also implies that aerosol particles within the boundary layer and within the mid-troposphere can be efficiently transported to the upper troposphere via deep convection. Aerosol concentrations at 13.5 km altitude increased by a factor of 7.71, 5.36, and 5.16, respectively, in the LAYER1, LAYER2, and LAYER3 cases, with a more notable effect when aerosol increased in the boundary layer (the LAYER1 case).

[28] A group of sensitivity tests were conducted to determine whether the results are robust to different aerosol conditions, in which aerosol layers added at different altitudes based on clean condition (the number concentrations of background aerosol for these tests were assumed to be 1/4 of CONTROL case). The results exhibited similar aerosol effect on updrafts, with significant enhanced vertical velocities occurred when aerosol layer existed at the boundary layer. In order to separate the effects of the vertical transport

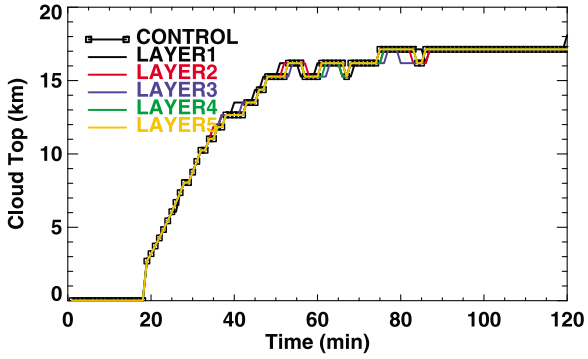

Figure 7. Time evolution of cloud top height in different cases.

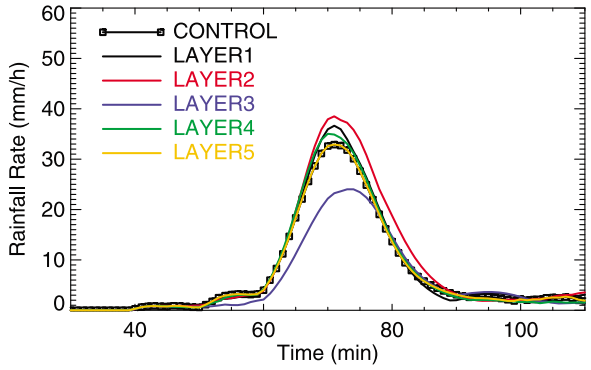

Figure 8. Time evolution of maximum precipitation rate in different cases.

scheme on the vertical distribution of aerosol particles, we also conducted separate sensitivity tests in which aerosol particles were added to the boundary layer (referred to as the LAYER1-a case) and the mid-troposphere (referred to as the LAYER2-a and LAYER3-a cases), without considering the feedback of aerosol layers on dynamic and microphysical processes. The results indicated a slightly weaker but still more efficient transport effect for the LAYER1-a case as compared to the LAYER2-a and LAYER3-a cases, consistent with the study of *Barthe et al.* [2011] who highlighted the importance of tracer transport into the upper troposphere from layers near the surface (0–1.5 km).

3.5. The Characteristics of the Particle Size Spectra at UT

[29] The averaged spectra of aerosol particles for all of the simulations at 120 min are presented in Figure 12. The vertical transport of aerosol particles larger than 0.01 μm in radius were examined in the present study (Figure 2a). In the CONTROL case, the number concentration of the Aitken mode and a part of the accumulation mode (0.1–0.2 μm) particles at UT (at 14.3 km altitude) increased as a result of convective transport (the solid line in Figure 12), and agreed with the studies of *Ekman et al.* [2006], *Hermann et al.* [2008], as well as *Tulet et al.* [2010], who demonstrated that particles smaller than 1 μm can reach the upper troposphere through deep convection due to inefficient scavenging. Aerosol particles at altitudes above the mid-troposphere (higher than 6.6 km) were significantly enhanced when an aerosol layer existed at the boundary layer (LAYER1) and in the mid-troposphere (LAYER2 and LAYER3), with a more notable effect found in the LAYER1 case (Figure 9). When aerosol layers were present at UT altitudes (cases LAYER4 and LAYER5), cloud and precipitation scavenging had little influence on the aerosol size distribution of their initial layers (Figures 12e and 12f). However, the number of particles smaller than 0.5 μm at an altitude above 12.6 km markedly increased in the LAYER4 case, due to the outflow of convection.

4. Summary and Conclusions

[30] Spectral bin microphysical schemes [*Tzivion et al.*, 1987; 1989; *Reisin et al.*, 1996; *Yin et al.*, 2005] were implemented into the cloud resolving model [*Tao et al.*,

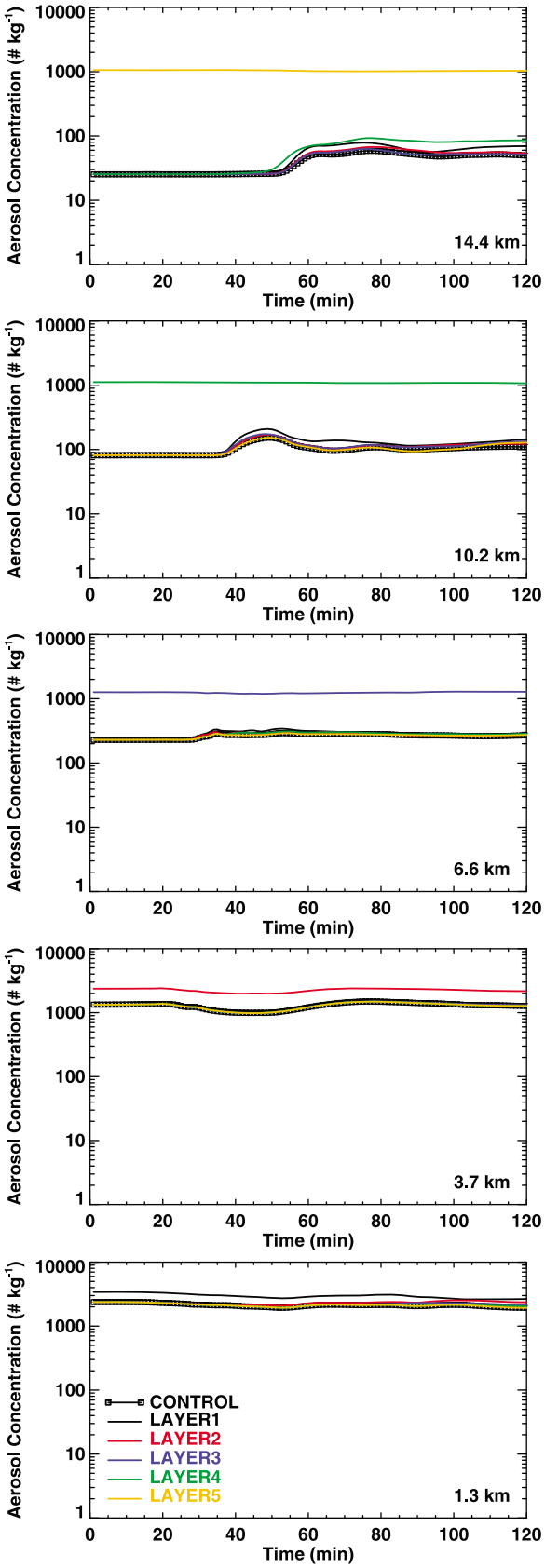

Figure 9. Time evolution of the average number concentration of aerosols at five altitudes (1.3 km, 3.7 km, 6.6 km, 10.2 km and 14.4 km) in different cases.

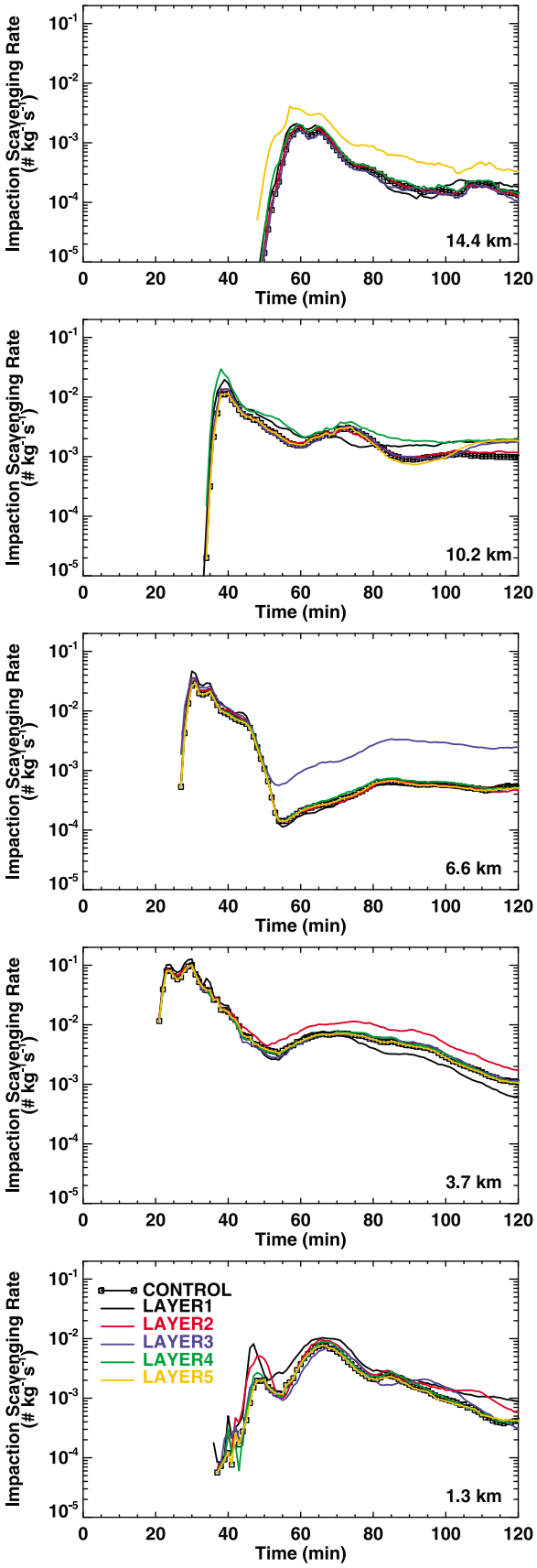

Figure 10. As in Figure 8, but for average impaction scavenging rate of aerosol particles.

2003] in order to investigate the effects of aerosol layers on cloud development and the vertical transport of aerosols by deep convection. The parameterization of ice formation proposed by *DeMott et al.* [2010] was used for the prediction of ice crystals. A convective cloud event that occurred on 1 December 2005 in Darwin, Australia was simulated using the coupled model, and was compared with available radar measurements. The results indicated that the main characteristics of the storm were well reproduced by the model, especially for the horizontal and vertical structure of the convective core.

[31] Aerosol layers located at five different altitudes were purposely added in order to understand how aerosols transported to the UT by deep convection are sensitive to the origin of aerosol layers, and the effect of aerosol layers on cloud development, as well as the dynamic structure of clouds. Sensitivity tests indicated that aerosol particles originating from the boundary layer (the LAYER1 case) can be transported upward more efficiently, as compared to those from the mid-troposphere, due to the significantly increased vertical velocity of the development stage of convection through the reinforced homogeneous freezing of droplets. Aerosol layers enhanced at altitudes above the boundary layer, i.e., cases LAYER2 to LAYER5, had little influence on cloud dynamic processes, but precipitation increased in most cases when an aerosol layer was present, except for the case when added aerosol appeared at 5.4–8.0 km (the LAYER3

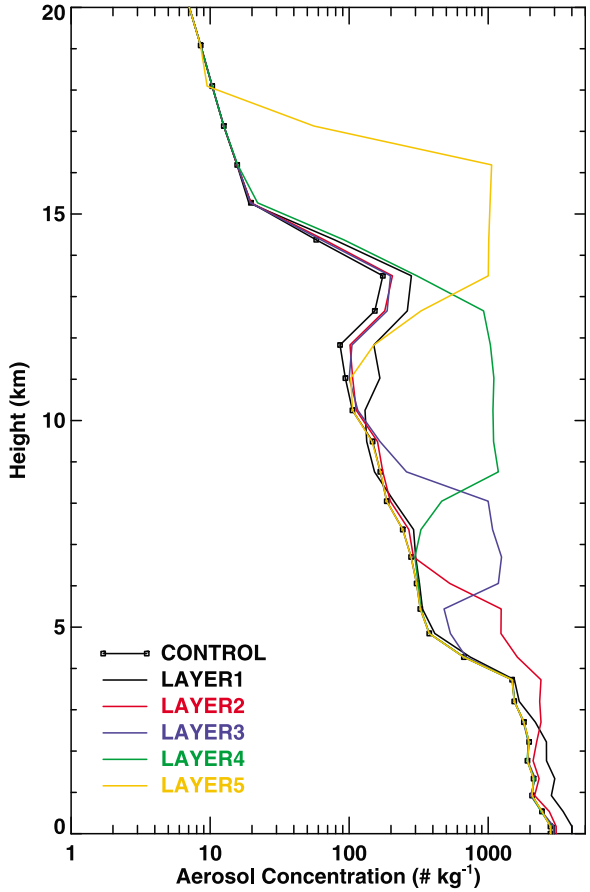

Figure 11. Vertical distribution of the concentration of aerosol particles at 75 min of simulation.

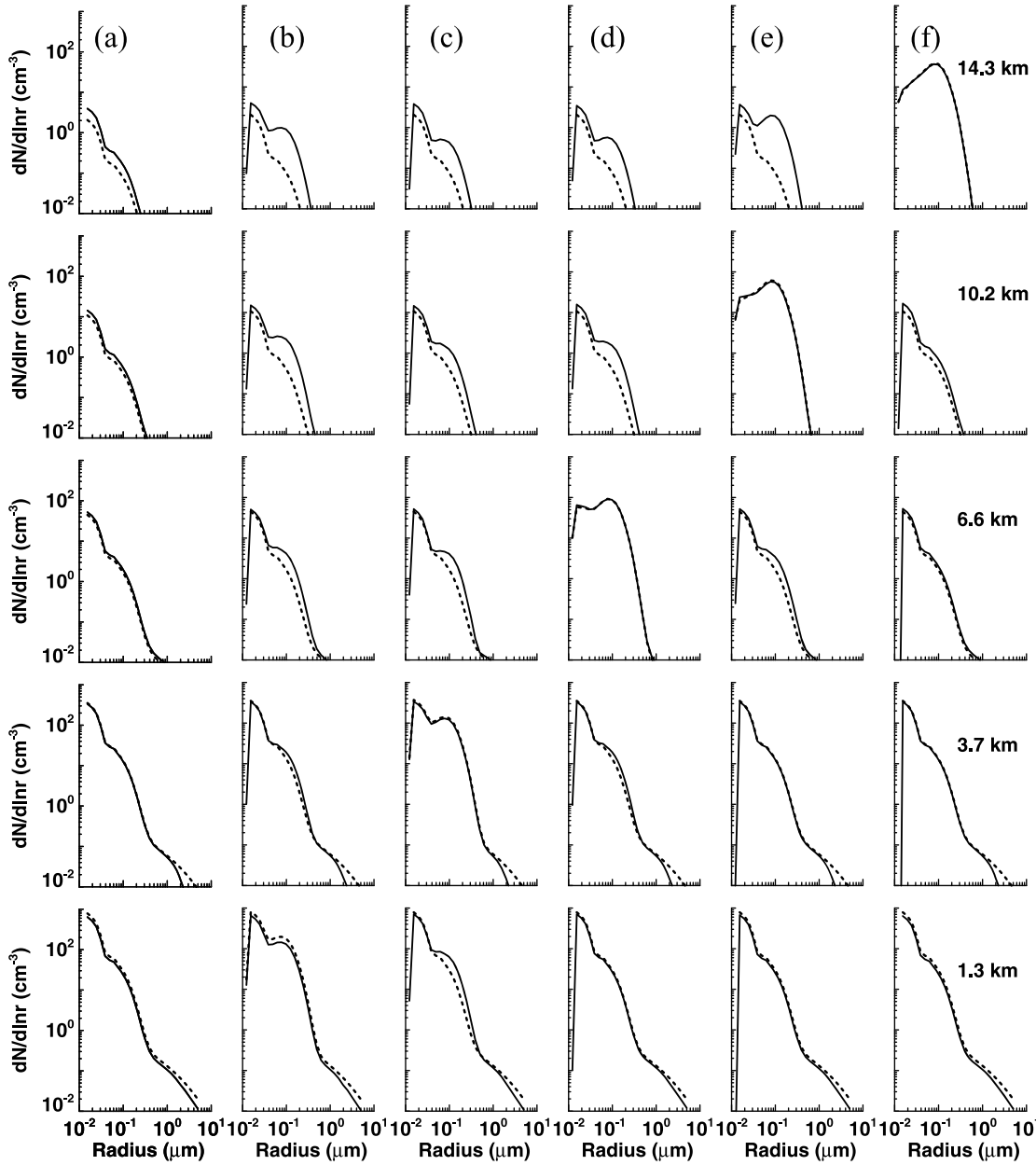

Figure 12. The average size distribution of aerosol particles at different altitudes at the initial time (dashed line) and 120 min of simulation (solid line) in case (a) CONTROL, (b) LAYER1, (c) LAYER2, (d) LAYER3, (e) LAYER4, and (f) LAYER5, respectively.

case). For this case, the smaller graupel mass resulted in less precipitation.

[32] For aerosol layers within the mid-troposphere, vertical profiles for aerosols exhibited two peaks as a result of cloud processing - one at the initial layer and the other at the altitude of 12–14 km. Aerosol concentrations at altitudes of 13.5 km were enlarged by factors of 7.71, 5.36, and 5.16 when the aerosol layer existed at 0–2.2 km, 2.2–5.4 km, and 5.4–8.0 km, respectively, and when the Aitken mode and a portion of accumulation mode (0.1–0.2 μm) particles could be transported to the UT. When the layer lofted to an altitude above 12.6 km, upward convective transport had almost no influence on the size distribution of aerosols at the initial level.

[33] The findings of this paper were limited to the specific parameterizations of sub-grid mixing used for the simulations. *Takemi and Rotunno* [2003] investigated the effects of sub-grid mixing in mesoscale cloud simulations, and pointed out that different choices of parameters in turbulence-closure schemes could affect the development of convective cloud. Since the upward transport of aerosols that we studied here may be sensitive to the evolution of vertical velocity over cloudy regions to some extent, further studies aimed at quantifying the uncertainties in the parameterizations are

needed. Moreover, the emphasis of the present study was based on the individual development of a convective cloud. Different cloud types, atmospheric thermodynamic conditions, as well as varied vertical velocities, may change the results due to complex aerosol-cloud interactions and the strong dependence of transport efficiency on updrafts, and should also be considered in future studies [*Ekman et al.*, 2007; *Fan et al.*, 2007].

[34] **Acknowledgments.** This study was jointly sponsored by the National Science Foundation of China (Grant 41030962), National Basic Research Program of China (Grant 2010CB428602), the Public Meteorology Special Foundation of MOST (Grant GYHY200706036), the Priority Academic Program of Development of Jiangsu Higher Education Institutions (PAPD), and the Program for Postgraduates Research and Innovation in Universities of Jiangsu Province (Grant CX09B_225Z).

References

Allen, G., et al. (2008), Aerosol and trace-gas measurements in the Darwin area during the wet season, *J. Geophys. Res.*, *113*, D06306, doi:10.1029/2007JD008706.

Andreae, M. O., et al. (2001), Transport of biomass burning smoke to the upper troposphere by deep convection in the equatorial region, *Geophys. Res. Lett.*, *28*, 951–954, doi:10.1029/2000GL012391.

Barthe, C., C. Mari, J. P. Chaboureau, P. Tulet, F. Roux, and J. P. Pinty (2011), Numerical study of tracers transport by a mesoscale convective system over West Africa, *Ann. Geophys.*, *29*(5), 731–747, doi:10.5194/angeo-29-731-2011.

Bryan, G. H., and H. Morrison (2012), Sensitivity of a simulated squall line to horizontal resolution and parameterization of microphysics, *Mon. Weather Rev.*, *140*(1), 202–225, doi:10.1175/MWR-D-11-00046.1.

Chen, B., and Y. Yin (2011), Modeling the impact of aerosols on tropical overshooting thunderstorms and stratospheric water vapor, *J. Geophys. Res.*, *116*, D19203, doi:10.1029/2011JD015591.

Chen, Q., Y. Yin, L.-J. Jin, H. Xiao, and S.-C. Zhu (2011), The effect of aerosol layers on convective cloud microphysics and precipitation, *Atmos. Res.*, *101*(1–2), 327–340, doi:10.1016/j.atmosres.2011.03.007.

Choi, Y.-S., C.-H. Ho, J. Kim, D.-Y. Gong, and R. J. Park (2008), The impact of aerosols on the summer rainfall frequency in China, *J. Appl. Meteorol. Climatol.*, *47*(6), 1802–1813, doi:10.1175/2007JAMC1745.1.

Christensen, M. W., and G. L. Stephens (2011), Microphysical and macrophysical responses of marine stratocumulus polluted by underlying ships: Evidence of cloud deepening, *J. Geophys. Res.*, *116*(D3), D03201, doi:10.1029/2010JD014638.

Cui, Z., and K. S. Carslaw (2006), Enhanced vertical transport efficiency of aerosol in convective clouds due to increases in tropospheric aerosol abundance, *J. Geophys. Res.*, *111*, D15212, doi:10.1029/2005JD006781.

de Reus, M., R. Krejci, J. Williams, H. Fischer, R. Scheele, and J. Ström (2001), Vertical and horizontal distributions of the aerosol number concentration and size distribution over the northern Indian Ocean, *J. Geophys. Res.*, *106*, 28,629–28,641, doi:10.1029/2001JD900017.

DeMott, P. J., A. J. Prenni, X. Liu, S. M. Kreidenweis, M. D. Petters, C. H. Twohy, M. S. Richardson, T. Eidhammer, and D. C. Rogers (2010), Predicting global atmospheric ice nuclei distributions and their impacts on climate, *Proc. Natl. Acad. Sci. U. S. A.*, *107*(25), 11,217–11,222, doi:10.1073/pnas.0910818107.

Devine, G. M., K. S. Carslaw, D. J. Parker, and J. C. Petch (2006), The influence of subgrid surface-layer variability on vertical transport of a chemical species in a convective environment, *Geophys. Res. Lett.*, *33*, L15807, doi:10.1029/2006GL025986.

Ekman, A. M. L., C. Wang, J. Ström, and R. Krejci (2006), Explicit simulation of aerosol physics in a cloud-resolving model: Aerosol transport and processing in the free troposphere, *J. Atmos. Sci.*, *63*(2), 682–696, doi:10.1175/JAS3645.1.

Ekman, A. M. L., C. Wang, J. Wilson, and J. Ström (2004), Explicit simulations of aerosol physics in a cloud-resolving model: A sensitivity study based on an observed convective cloud, *Atmos. Chem. Phys.*, *4*(3), 773–791, doi:10.5194/acp-4-773-2004.

Ekman, A. M. L., A. Engström, and C. Wang (2007), The effect of aerosol composition and concentration on the development and anvil properties of a continental deep convective cloud, *Q. J. R. Meteorol. Soc.*, *133*(627), 1439–1452, doi:10.1002/qj.108.

Fan, J., R. Zhang, G. Li, and W.-K. Tao (2007), Effects of aerosols and relative humidity on cumulus clouds, *J. Geophys. Res.*, *112*, D14204, doi:10.1029/2006JD008136.

Fan, J., J. M. Comstock, and M. Ovchinnikov (2010), The cloud condensation nuclei and ice nuclei effects on tropical anvil characteristics and water vapor of the tropical tropopause layer, *Environ. Res. Lett.*, *5*(4), 044005, doi:10.1088/1748-9326/5/4/044005.

Fan, J., L. R. Leung, Z. Li, H. Morrison, H. Chen, Y. Zhou, Y. Qian, and Y. Wang (2012), Aerosol impacts on clouds and precipitation in eastern China: Results from bin and bulk microphysics, *J. Geophys. Res.*, *117*, D00K36, doi:10.1029/2011JD016537.

Feingold, G., S. Tzivion, and Z. Leviv (1988), Evolution of raindrop spectra. Part I: Solution to the stochastic collection/breakup equation using the method of moments, *J. Atmos. Sci.*, *45*(22), 3387–3399, doi:10.1175/1520-0469(1988)045<3387:EORSPI>2.0.CO;2.

Fierli, F., E. Orlandi, K. S. Law, C. Cagnazzo, F. Cairo, C. Schiller, S. Borrmann, G. Di Donfrancesco, F. Ravegnani, and C. M. Volk (2011), Impact of deep convection in the tropical tropopause layer in West Africa: In-situ observations and mesoscale modelling, *Atmos. Chem. Phys.*, *11*(1), 201–214, doi:10.5194/acp-11-201-2011.

Froyd, K. D., D. M. Murphy, T. J. Sanford, D. S. Thomson, J. C. Wilson, L. Pfister, and L. Lait (2009), Aerosol composition of the tropical upper troposphere, *Atmos. Chem. Phys.*, *9*(13), 4363–4385, doi:10.5194/acp-9-4363-2009.

Heald, C. L., D. J. Jacob, R. J. Park, B. Alexander, T. D. Fairlie, R. M. Yantosca, and D. A. Chu (2006), Transpacific transport of Asian anthropogenic aerosols and its impact on surface air quality in the United States, *J. Geophys. Res.*, *111*, D14310, doi:10.1029/2005JD006847.

Hermann, M., C. A. M. Brenninkmeijer, F. Slemr, J. Heintzenberg, B. G. Martinsson, H. Schlager, P. F. J. V. Velthoven, A. Wiedensohler, A. Zahn, and H. Ziereis (2008), Submicrometer aerosol particle distributions in the upper troposphere over the mid-latitude North Atlantic—Results from the third route of 'CARIBIC', *Tellus, Ser. B*, *60*(1), 106–117, doi:10.1111/j.1600-0889.2007.00323.x.

Johnson, D. E., W. K. Tao, J. Simpson, and C. H. Sui (2002), A study of the response of deep tropical clouds to large-scale thermodynamic forcings. Part I: Modeling strategies and simulations of TOGA COARE convective systems, *J. Atmos. Sci.*, *59*(24), 3492–3518, doi:10.1175/1520-0469(2002)059<3492:ASOTRO>2.0.CO;2.

Khain, A., and A. Pokrovsky (2004), Simulation of effects of atmospheric aerosols on deep turbulent convective clouds using a spectral microphysics mixed-phase cumulus cloud model. Part II: Sensitivity study, *J. Atmos. Sci.*, *61*(24), 2983–3001, doi:10.1175/JAS-3281.1.

Klemp, J. B., and R. B. Wilhelmson (1978), The simulation of three-dimensional convective storm dynamics, *J. Atmos. Sci.*, *35*(6), 1070–1096, doi:10.1175/1520-0469(1978)035<1070:TSOTDC>2.0.CO;2.

Lebo, Z. J., and J. H. Seinfeld (2011), Theoretical basis for convective invigoration due to increased aerosol concentration, *Atmos. Chem. Phys.*, *11*(11), 5407–5429, doi:10.5194/acp-11-5407-2011.

Lee, S.-S., and G. Feingold (2010), Precipitating cloud-system response to aerosol perturbations, *Geophys. Res. Lett.*, *37*(23), L23806, doi:10.1029/2010GL045596.

Lee, S. S., L. J. Donner, V. T. J. Phillips, and Y. Ming (2008), The dependence of aerosol effects on clouds and precipitation on cloud-system organization, shear and stability, *J. Geophys. Res.*, *113*, D16202, doi:10.1029/2007JD009224.

Lee, S. S., J. E. Penner, and S. M. Saleeby (2009), Aerosol effects on liquid-water path of thin stratocumulus clouds, *J. Geophys. Res.*, *114*(D7), D07204, doi:10.1029/2008JD010513.

Li, G., Y. Wang, and R. Zhang (2008), Implementation of a two-moment bulk microphysics scheme to the WRF model to investigate aerosol-cloud interaction, *J. Geophys. Res.*, *113*, D15211, doi:10.1029/2007JD009361.

Martins, J. A., M. A. F. Silva Dias, and F. L. T. Goncalves (2009), Impact of biomass burning aerosols on precipitation in the Amazon: A modeling case study, *J. Geophys. Res.*, *114*, D02207, doi:10.1029/2007JD009587.

Ntelekos, A. A., J. A. Smith, L. Donner, J. D. Fast, W. I. Gustafson, E. G. Chapman, and W. F. Krajewski (2009), The effects of aerosols on intense convective precipitation in the northeastern United States, *Q. J. R. Meteorol. Soc.*, *135*(643), 1367–1391, doi:10.1002/qj.476.

Pruppacher, H. R., and J. D. Klett (1997), *Microphysics of Clouds and Precipitation*, Kluwer Acad., Amsterdam.

Qu, P. (2009), Observational studies on carbon monoxide, ozone and aerosols in the troposphere of Darwin, Australia [in Chinese], MS thesis, School of Atmos. Phys., Nanjing Univ. of Inf. Sci. and Technol., Nanjing, China.

Reisin, T., Z. Levin, and S. Tzivion (1996), Rain production in convective clouds as simulated in an axisymmetric model with detailed microphysics. Part I: Description of the model, *J. Atmos. Sci.*, *53*(3), 497–519, doi:10.1175/1520-0469(1996)053<0497:RPICCA>2.0.CO;2.

Roberts, G., G. Mauger, O. Hadley, and V. Ramanathan (2006), North American and Asian aerosols over the eastern Pacific Ocean and their role

in regulating cloud condensation nuclei, *J. Geophys. Res.*, *111*, D13205, doi:10.1029/2005JD006661.

Schafer, R., P. T. May, T. D. Keenan, K. McGuffie, W. L. Ecklund, P. E. Johnston, and K. S. Gage (2001), Boundary layer development over a tropical island during the Maritime Continent Thunderstorm Experiment, *J. Atmos. Sci.*, *58*(15), 2163–2179, doi:10.1175/1520-0469(2001)058<2163:BLDOAT>2.0.CO;2.

Shepherd, T. G. (2007), Transport in the middle atmosphere, *J. Meteorol. Soc. Jpn.*, *85B*, 165–191, doi:10.2151/jmsj.85B.165.

Soong, S. T., and Y. Ogura (1980), Response of tradewind cumuli to large-scale processes, *J. Atmos. Sci.*, *37*(9), 2035–2050, doi:10.1175/1520-0469(1980)037<2035:ROTCTL>2.0.CO;2.

Soong, S. T., and W. K. Tao (1980), Response of deep tropical cumulus clouds to mesoscale processes, *J. Atmos. Sci.*, *37*(9), 2016–2034, doi:10.1175/1520-0469(1980)037<2016:RODTCC>2.0.CO;2.

Stith, J. L., et al. (2009), An overview of aircraft observations from the Pacific Dust Experiment campaign, *J. Geophys. Res.*, *114*, D05207, doi:10.1029/2008JD010924.

Su, H., J. H. Jiang, X. Liu, J. E. Penner, W. G. Read, S. Massie, M. R. Schoeberl, P. Colarco, N. J. Livesey, and M. L. Santee (2011), Observed increase of TTL temperature and water vapor in polluted clouds over Asia, *J. Clim.*, *24*(11), 2728–2736, doi:10.1175/2010JCLI3749.1.

Takemi, T., and R. Rotunno (2003), The effects of subgrid model mixing and numerical filtering in simulations of mesoscale cloud systems, *Mon. Weather Rev.*, *131*, 2085–2101, doi:10.1175/1520-0493(2003)131<2085:TEOSMM>2.0.CO;2.

Tao, W.-K., and J. Simpson (1993), Goddard Cumulus Ensemble Model. Part I: Model description, *Terr. Atmos. Oceanic Sci.*, *4*(1), 19–54.

Tao, W. K., et al. (2003), Microphysics, radiation and surface processes in the Goddard Cumulus Ensemble (GCE) model, *Meteorol. Atmos. Phys.*, *82*(1–4), 97–137, doi:10.1007/s00703-001-0594-7.

Tsai, F., G. T.-J. Chen, T.-H. Liu, W.-D. Lin, and J.-Y. Tu (2008), Characterizing the transport pathways of Asian dust, *J. Geophys. Res.*, *113*, D17311, doi:10.1029/2007JD009674.

Tulet, P., K. Crahan-Kaku, M. Leriche, B. Aouizerats, and S. Crumeyrolle (2010), Mixing of dust aerosols into a mesoscale convective system: Generation, filtering and possible feedbacks on ice anvils, *Atmos. Res.*, *96*(2–3), 302–314, doi:10.1016/j.atmosres.2009.09.011.

Tzivion, S., G. Feingold, and Z. Levin (1987), An efficient numerical solution to the stochastic collection equation, *J. Atmos. Sci.*, *44*(21), 3139–3149, doi:10.1175/1520-0469(1987)044<3139:AENSTT>2.0.CO;2.

Tzivion, S., G. Feingold, and Z. Levin (1989), The evolution of raindrop spectra. Part II: Collisional collection/breakup and evaporation in a rain-shaft, *J. Atmos. Sci.*, *46*(21), 3312–3328, doi:10.1175/1520-0469(1989)046<3312:TEORSP>2.0.CO;2.

Vernier, J. P., L. W. Thomason, and J. Kar (2011), CALIPSO detection of an Asian tropopause aerosol layer, *Geophys. Res. Lett.*, *38*, L07804, doi:10.1029/2010GL046614.

Wang, C. (2005a), A modeling study of the response of tropical deep convection to the increase of cloud condensation nuclei concentration: 2. Radiation and tropospheric chemistry, *J. Geophys. Res.*, *110*, D22204, doi:10.1029/2005JD005829.

Wang, C. (2005b), A modeling study of the response of tropical deep convection to the increase of cloud condensation nuclei concentration: 1. Dynamics and microphysics, *J. Geophys. Res.*, *110*, D21211, doi:10.1029/2004JD005720.

Wu, L., H. Su, and J. H. Jiang (2011), Regional simulations of deep convection and biomass burning over South America: 2. Biomass burning aerosol effects on clouds and precipitation, *J. Geophys. Res.*, *116*, D17209, doi:10.1029/2011JD016106.

Yin, Y., Z. Levin, T. G. Reisin, and S. Tzivion (2000), The effects of giant cloud condensation nuclei on the development of precipitation in convective clouds–a numerical study, *Atmos. Res.*, *53*(1–3), 91–116, doi:10.1016/S0169-8095(99)00046-0.

Yin, Y., S. Wurzler, Z. Levin, and T. G. Reisin (2002), Interactions of mineral dust particles and clouds: Effects on precipitation and cloud optical properties, *J. Geophys. Res.*, *107*(D23), 4724, doi:10.1029/2001JD001544.

Yin, Y., K. S. Carslaw, and G. Feingold (2005), Vertical transport and processing of aerosols in a mixed-phase convective cloud and the feedback on cloud development, *Q. J. R. Meteorol. Soc.*, *131*(605), 221–245, doi:10.1256/qj.03.186.

Zhang, H., G. M. McFarquhar, W. R. Cotton, and Y. Deng (2009), Direct and indirect impacts of Saharan dust acting as cloud condensation nuclei on tropical cyclone eyewall development, *Geophys. Res. Lett.*, *36*(6), L06802, doi:10.1029/2009GL037276.

Zhang, Y., S. Kreidenweis, and G. R. Taylor (1998), The effects of clouds on aerosol and chemical species production and distribution. Part III: Aerosol model description and sensitivity analysis, *J. Atmos. Sci.*, *55*(6), 921–939, doi:10.1175/1520-0469(1998)055<0921:TEOCOA>2.0.CO;2.